Efficient Electrically Small Antenna Facilitated by a Near-Field Resonant Parasitic

Richard W. Ziolkowski, *Fellow, IEEE*

***Abstract*—An electrically small electric-based metamaterial-inspired antenna system that is designed for narrow bandwidth operation near 300 MHz is presented. It consists of a lumped element-based resonant parasitic element that is introduced into the very near field of a coax-fed monopole. It is demonstrated that several idealized lossless versions are capable of achieving a near perfect impedance match to the source and, thus, have overall efficiencies near 100% without an external matching circuit. It is established that the entire system makes effective use of the radian-sphere volume it occupies. The overall efficiencies are shown to remain high even when conductor losses are introduced. Potential frequency agility is also demonstrated.**

***Index Terms*—Antenna efficiency, antenna theory, electrically small antennas, metamaterials, parasitic antennas, Q factor.**

I. Introduction

SEVERAL efficient electrically small antenna (ESA) systems have now been demonstrated theoretically using metamaterial constructs [1] and practically with metamaterial-inspired near-field parasitics, the EZ antennas reported in [2]. Another 3D electric-based version, the Z antenna, was introduced in [3]. In these designs, the presence of an electrically small resonant parasitic whose effective material properties were properly matched to the bare electrically small radiator led to near perfect reactive *and* resistive matching to the source without the introduction of an external matching circuit. The resulting electrically small resonant (electric-based) or anti-resonant (magnetic-based) antennas were demonstrated to have high overall efficiencies. Because of the sequence of antenna designs given in [1]–[3], it appears that the main facilitator to an efficient ESA is simply a resonant near-field parasitic. To test this hypothesis and, if positive, to answer the question of how small and how simple the near-field parasitic might be, were the central questions posed in this theoretical and numerical study. All simulations were performed with ANSOFT's High Frequency Structure Simulator, i.e., HFSS.

Because of the very small physical sizes relative to the wavelength and because of the desire to investigate very narrow bandwidth behaviors, the HFSS simulations were challenging. They were run on a 64-bit platform with HFSS v.11.0.2. The radiation boundary surfaces, as recommended by ANSOFT, were set slightly larger than $\lambda_{\rm res}/4$ away from the antenna system. The minimum convergence parameter was set at $\Delta S = 1.0 \times 10^{-4}$ to achieve adequate mesh resolution to obtain the necessary frequency resolution of the responses. All of the conductor volumes were pre-meshed to improve convergence. The radiation boundary surface was also pre-meshed to obtain the most accurate overall efficiency values. The lumped element was modeled with its actual dimensions, related materials properties, and an HFSS lumped RLC boundary element, which can be used to represent any combination of lumped resistor, inductor, and/or capacitor in parallel on a surface. This surface was centered in the physical model of the lumped element. The metal objects were modeled with real copper having $\sigma_{\rm copper} = 5.8 \times 10^7$ Siemens/m. When endcaps were included on the lumped element inductor, they were treated for comparison purposes either as lossless tin with an idealized conductivity $\sigma_{\rm tin,ideal} = 9.17 \times 10^{16}$ Siemens/m or as real tin with conductivity $\sigma_{\rm tin} = 9.17 \times 10^6$ Siemens/m.

II. Resonant Near-Field Parasitic Antenna Design

The geometry of the monopole, near-field parasitic system is shown in Fig. 1 along with definitions of its dimensions. The circular wire monopole is coaxially fed through a ground plane (the xy-plane in Fig. 1) and has the same radius as the inner conductor of the coax, $\rm r_w = 0.3\ mm$. The outer radius of the coax is set to $\rm b = 2.301\ r_w = 0.6903\ mm$ to achieve a 50 Ω feedline. The height of the monopole was $\rm H1 = 0.85\ mm$. The HFSS predicted impedance of the coax was 49.975 Ω. The bare monopole with ideal copper produced a total radiated power $\rm P_{rad} = 1.16 \times 10^{-9}\ W$ for an input power $\rm P_{in} = 1.0\ W$ because its input impedance $\rm Z_{in} = 1.16 \times 10^{-9} - j\ 10540\ \Omega$ was very poorly matched to the source.

There is a wide variety of design options available to match such an electrically small antenna to the source. The most common is an external matching circuit, e.g., an inductor of the appropriate value is connected directly to the monopole to achieve conjugate matching and then a quarter-wavelength transformer is introduced to achieve resistive matching. The resonant parasitic element is a different paradigm. It represents an internal matching element; yet it is part of the antenna itself since it contributes to the radiation process. It may be advantageous because now the entire antenna system is electrically small, yet matched to the source without any external contrivances.

The near-field parasitic consisted of a rectangular parallelpiped inductor connected to a conductive wire of the same shape. The dimensions of the lumped element model (lower portion of parasitic) were based on those corresponding to

Manuscript received March 24, 2008; revised April 25, 2008. First published May 16, 2008; current version published December 19, 2008 This work was supported in part by DARPA under Contract HR0011-05-C-0068.

The author is with the Department of Electrical and Computer Engineering, University of Arizona, Tucson, AZ 85721-0104 USA (e-mail: ziolkowski@ece.arizona.edu).

Color versions of one or more of the figures in this letter are available online at http://ieeexplore.ieee.org.

Digital Object Identifier 10.1109/LAWP.2008.2000558

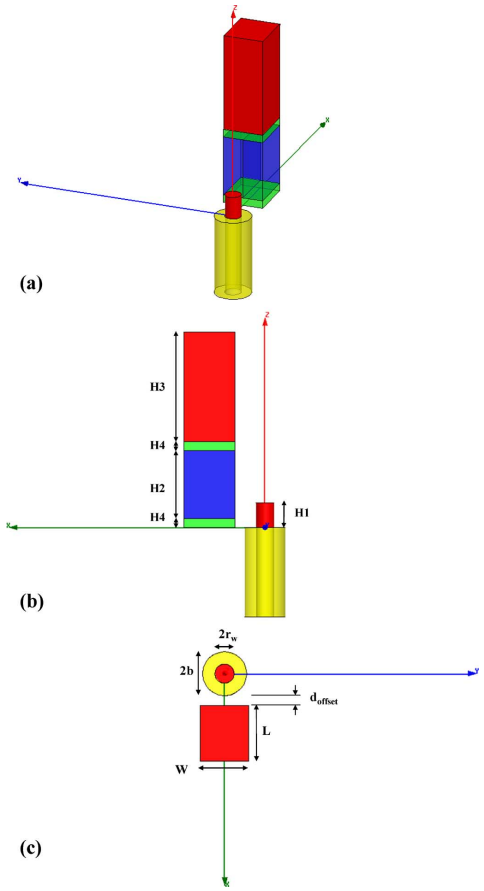

Fig. 1. The antenna system and its dimensions (a) 3D view, (b) side view, and (c) top view. The ground plane is located in the xy-plane.

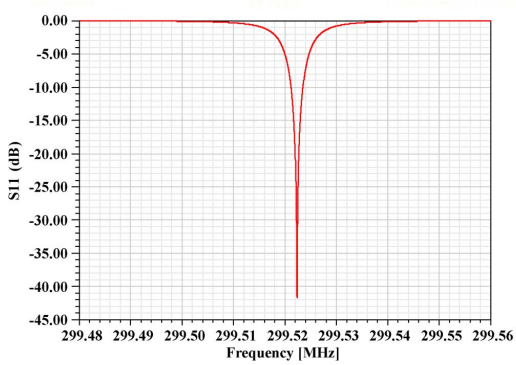

Fig. 2. HFSS predicted S_{11} values.

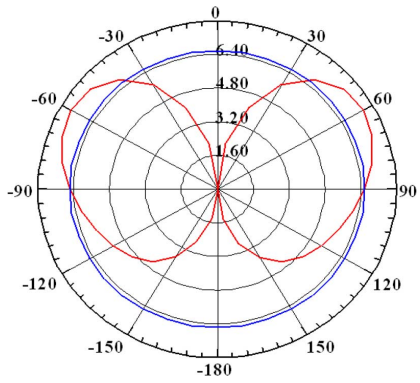

Fig. 3. HFSS predicted E- and H- plane far field patterns.

the API Delevan Series 0805 wire-wound surface mount inductor [4] that was used in [3]. This means $\mathrm{L} = 1.73\ \mathrm{mm}$, $\mathrm{W} = 1.52\ \mathrm{mm}$, and $\mathrm{H2} = 2.29\ \mathrm{mm}$. The HFSS RLC element was oriented radially away from the wire (in zx-plane). A metallic arm (upper portion of parasitic) was attached to the inductor and oriented vertically. It has the dimensions L, W, and $\mathrm{H3} = 3.7\ \mathrm{mm}$. Two rectangular discs were inserted to represent its endcaps: one between the ground plane and the inductor, and one between the inductor and the conductor arm of the parasitic. The endcaps were set to L, W, and $\mathrm{H4} = 0.3\ \mathrm{mm}$. Consequently, the total height of the parasitic was 6.59 mm. The center of the edge of the parasitic was offset from outer wall of the coax a distance $\mathrm{d_{offset}} = 0.3097\ \mathrm{mm}$, i.e., the edge of the parasitic was 1.0 mm from the center of the monopole. The RLC element produced the specified inductance value. However, because its electromagnetic properties were not known exactly, the inductor's casing material was treated as an ideal dielectric. In this case, the casing was approximated as a dielectric with relative permittivity $\varepsilon_{\mathrm{r}} = 2.2$. Consequently, the inductor was modeled as an idealized lossless element.

It was desired to achieve a resonance near 300 MHz. This choice was made simply to have the free space wavelength approximately 1.0 m. With the indicated dimensions, real copper for the monopole and the parasitic arm, idealized tin for the endcaps, and with the inductor value $\mathrm{L_{ind}} = 1300\ \mathrm{nH}$, the resonant frequency was $\mathrm{f_{res}} = 299.52231\ \mathrm{MHz}$. The HFSS predicted $\mathrm{S_{11}}$ values are given in Fig. 2 and show near complete matching to the source at the resonance frequency. The overall radiated power was $\mathrm{P_{rad}} = 0.972\ \mathrm{W}$. The S-parameter and the total radiated power values clearly demonstrate that the resonant parasitic acts like an internal matching circuit for the antenna. As with the Z antenna in [3], the radiation patterns of this antenna system, shown in Fig. 3, have the same form as the bare monopole, i.e., a monopole in the presence of a truncated ground plane, but with a much larger amplitude corresponding to the much improved overall efficiency of the system. In comparison, when the endcaps were treated as real tin, the overall radiated power was reduced to $\mathrm{P_{rad}} = 0.840\ \mathrm{W}$; as copper, $\mathrm{P_{rad}} = 0.915\ \mathrm{W}$. These results emphasize the need for a complete understanding of all of the material properties, particularly those of the inductor, to achieve the best practical design.

Why is the parasitic considered as a resonant element? This is illustrated in Fig. 4 with circuit and transmission line equivalents for the electromagnetic objects. Because the parasitic arm is also an electrically small radiator, it too acts as a capacitive element. This capacitor is connected to the lumped element inductor in series and the current path is closed by the displacement current, as it is for the monopole itself. The entire parasitic thus forms an LC resonant element and radiates as a monopole. The formula for the input impedance of an electrically small monopole follows immediately from the dipole result [5] as

$$Z_{\mathrm{input}}^{\mathrm{monopole}} = 40\pi^2\left(\frac{h_a}{\lambda}\right)^2 - j60\frac{\ln(h_a/r_a)-1}{\tan(2\pi h_a/\lambda)}$$

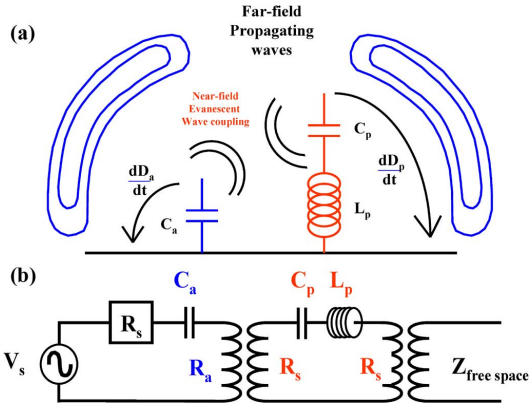

Fig. 4. Equivalent models of the antenna system (a) Fields and elements, (b) transmission line.

$$= R_a + jX_a = R_a - j\frac{1}{\omega C_a} \tag{1}$$

where h_a is the height of the monopole and r_a is its radius. Using (1) to calculate the effective capacitance of the monopole, $\mathrm{C_a}$, and of the parasitic element, $\mathrm{C_p}$ (taking into account its entire height and its smallest transverse dimension to determine its radius) and then adding them in series as indicated in Fig. 4, the resonant frequency of the circuit model is approximately

$$f_{\mathrm{res}} \approx \frac{1}{2\pi}\sqrt{\frac{C_p + C_a}{L_p(C_pC_a)}} = 280.72\ \mathrm{MHz} \tag{2}$$

where $\mathrm{L_p}$ is the inductance of the lumped element, the dominant inductive contribution in this system. This result is in reasonable agreement with the value obtained with the detailed HFSS calculations. The parasitic element causes the total reactance in Fig. 4 to be zero at the resonance frequency. However, this result does not reflect its other major function.

The resonant parasitic element also acts as an impedance transformer. It not only provides matching of the antenna to the source, but it also provides the requisite matching to free space. It is a transducer that converts the strong evanescent fields of the monopole into propagating waves. The second impedance transformer in Fig. 4(b) is meant to represent explicitly this overall function of the antenna system, a transducer of the electrical power in the interior of its radiansphere to electromagnetic power in its exterior. It is also clear from these arguments how the geometrical and physical parameters interact. For example, if the height of the monopole or the parasitic element is reduced, the capacitance is increased. A smaller inductor value would then be necessary to maintain the same resonance frequency. For a given resonant parasitic, matching can usually be achieved simply by adjusting the height of the monopole appropriately. Guided by such basic precepts, this initial design and several alternatives were obtained with only a few numerical iterations.

From Fig. 2 it is clear that the antenna system has a very narrow bandwidth. The half power (VSWR) fractional bandwidth was $\mathrm{FBW} = 2.32\times10^{-5}$, giving $\mathrm{Q} = 2/\mathrm{FBW} = 8.62\times 10^{+4}$. The radius of the minimum enclosing sphere is taken to be the radius from the center of the parasitic to its top corner, $\mathrm{a} = 6.647\ \mathrm{mm}$. Then, at the resonance frequency $\mathrm{ka} = 0.0417$ and

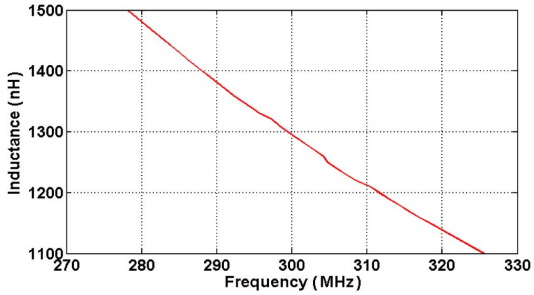

Fig. 5. Resonant frequency values for changing inductor values.

$\lambda/\mathrm{a} \sim 151$. The corresponding Chu lower bound quality factor, including the radiation efficiency [6], gives $\mathrm{Q_{lb}} = 1.34\times10^{+4}$ and, hence, $\mathrm{Q} = 6.42\ \mathrm{Q_{lb}}$. Note, however, that the entire antenna is not filling the radian hemisphere surrounding it. In fact, if the effective volume of the antenna is taken to be the volume of the rectangular parallelpiped enclosing the far edge of the coax and the entire parasitic: $4.1106\ \mathrm{mm}\times1.52\ \mathrm{mm}\times6.59\ \mathrm{mm}$, the ratio of volume of the radian hemisphere enclosing the antenna, $2\pi\mathrm{a}^3/3$, to this antenna volume is 14.94. The monopole and the near-field parasitic system is making very efficient use of its effective volume.

The variation in the resonance frequency as a function of the inductor values was also considered. The resonant frequency at each 10 nH step from 1150 nH to 1450 nH, as well as at the endpoints: 1100 nH and 1500 nH, were obtained simply by changing the inductor value and searching for the resonance with fast sweeps, making sure that the minimum $\mathrm{S_{11}}$ value was below -40 dB. The HFSS predicted results are shown in Fig. 5.

In all cases the HFSS simulations predicted that the total radiated power was $\mathrm{P_{rad}} \sim 0.97\ \mathrm{W}$ (there were small variations in the third decimal place). It is quite interesting that the near-field resonant parasitic is a robust matching element despite it being very electrically small. As with the Z antenna, a frequency agile and possibly a broad instantaneous bandwidth system may be possible by replacing the inductor with an active (non-Foster) internal matching circuit [7]. The present configuration would have an immediate advantage over the Z antenna because the inductor region could be accessed directly from below the ground plane.

III. Alternate Designs

With this initial success, there were questions as to what would happen with changes in the geometry. For instance, the effect of the location of the parasitic was considered. Moving the parasitic further away from (closer to) the monopole lowered (raised) the resonant frequency. Moving the edge of the parasitic to 2.5 mm from the monopole center (1.8097 mm from the outer conductor of the coax), it was found that the resonance frequency was lowered to 295.73325 MHz with $\mathrm{P_{rad}} = 0.973\ \mathrm{W}$. Changing the length of the parasitic required changing the length of the monopole to re-establish matching. Nonetheless, complete matching and approximately the same overall efficiency was maintained.

Other variations based on practical considerations were also simulated. For example, ECM electronics sells an axial molded choke, model MF1303T-1R2, that has a 1200 nH

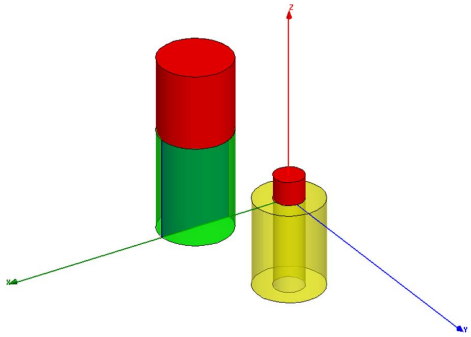

Fig. 6. Circular inductor version of the near-field parasitic. The ground plane is located in the xy-plane.

inductance value [8]. The length of the main body of this inductor is 3.35 mm, its diameter is 2.41 mm, and its axial wire radius is 0.5 mm. This inductor was used as the basis for the parasitic system shown in Fig. 6. It has an epoxy casing which was modeled with the epoxy Kevlar values in the HFSS data base: $\varepsilon_r = 3.6$, $\mu_r = 1.0$, and negligible loss tangents. The parasitic arm was made cylindrical to fit exactly on the inductor. Its height was 2.5 mm. Thus the overall height of the parasitic was 5.85 mm, giving $a = 5.9728$ mm. To have the same wire dimensions, the monopole radius was increased to $r_a = 0.5$ mm. This increased the outer radius of the coax to $b = 1.1505$ mm. The simulated coax impedance was 49.964 Ω. The antenna length was $H1 = 0.8$ mm. The ground plane is located in the xy-plane of Fig. 6. The offset distance between the outer edge of the coax and the outer edge of the parasitic was $d_{offset} = 1.0$ mm. No solder discs were included because the parasitic could be assembled with the inductor wire soldered to the ground plane and the parasitic arm attached snug-fit to the inductor wire. The HFSS predicted resonance frequency was $f_{res} = 290.3885$ MHz ($S_{11} = -48.9$ dB). This gives $ka = 0.036$ and $\lambda/a \sim 173$. The total radiated power was 0.970 W. The quality factor was $Q = 4.29\ Q_{lb}$. This design makes even more effective use of its radiating volume; and it would probably be the most practical to try experimentally.

Yet another design was considered that was based on the 1500 nH version of the Murata magnetically shielded monolithic inductor LQM21N [9]. This choice was made because its design actually matches the model shown in Fig. 1, but with smaller dimensions. In particular, $L = 1.25$ mm, $W = 0.85$ mm, and $H2 = 2.0$ mm. With $r_a = 0.3$ mm, $H1 = 0.74$ mm, $d_{offset} = 2.0$ mm, and $H3 = 3.4$ mm, the HFSS predicted resonance frequency was $f_{res} = 298.3885$ MHz ($S_{11} = -46.4$ dB). This gives $ka = 0.034$ and $\lambda/a \sim 184$. The total radiated power was 0.826 W. The quality factor was $Q = 7.28\ Q_{lb}$.

These design variations demonstrate the robustness of the basic concept. The cylindrical version, being about the same size, maintained the same overall efficiency. While the smaller version showed a decrease in the overall efficiency, its predicted value remains interesting.

IV. Conclusion

An efficient electrically small antenna system was introduced and its performance was characterized numerically. By introducing a resonant lumped element-based parasitic element into the very near field of a coax-fed monopole, near complete impedance matching to the source and efficient coupling to free space was enabled. Several variations of the design were presented and their performance characteristics were compared. Despite being very electrically small, the overall efficiencies were predicted to be very high. This near-field resonant parasitic appears to an advantage over directly loading the radiating element with a conjugate matching element and introducing some type of external resistive matching circuit because it provides internally not only the same reactance matching, but it also furnishes the requisite resistance matching—without the need to introduce any external circuit elements. The configuration is analogous to a dielectric resonator antenna; but it, like the metamaterial-based and -inspired antenna systems, is enabled through the realization of a highly subwavelength-sized resonator. Such a resonator is enabled at the low frequencies considered here by the lumped element; at higher frequencies one would again have to deal with metamaterial constructs or some inspired analogue. A frequency agile system could be realized by simply changing the inductance of the parasitic. Active internal matching network approaches are under consideration to achieve larger instantaneous bandwidth.

Experiments to confirm the simulation results reported here are being planned. As already noted, a critical issue that could significantly impact the overall system performance is the actual electromagnetic behavior of the inductor. While an inductor's circuit values are provided by its supplier, its electromagnetic properties are not. In addition to metallic losses in the inductor itself (i.e., finite Q values), simulations indicate that field losses in the inductor casing material can significantly impact the overall efficiency. Experimental data could lead to desirable improvements in the simulation models and their predicted results.

References

[1] R. W. Ziolkowski and A. Erentok, "Metamaterial-based efficient electrically small antennas," *IEEE Trans. Antennas Propag.*, vol. 54, pp. 2113–2130, Jul. 2006.

[2] A. Erentok and R. W. Ziolkowski, "Metamaterial-inspired efficient electrically small antennas," *IEEE Trans. Antennas Propag.*, vol. 56, pp. 691–707, Mar. 2008.

[3] R. W. Ziolkowski, "An efficient, electrically small antenna designed for VHF and UHF applications," *IEEE Antennas Wireless Propag. Lett.*, vol. 7, pp. 217–220, Mar. 2008.

[4] API Delevan, "Series 0805R Wire-Wound Surface Mount Inductor Data Sheet," p. 12 [Online]. Available: http://www.delevan.com, (08/09/2007)

[5] C. A. Balanis, *Antenna Theory*, 3rd ed. New York: Wiley, 2005, p. 640.

[6] S. R. Best, "Low Q electrically small linear and elliptical polarized spherical dipole antennas," vol. 53, pp. 1047–1053, Mar. 2005.

[7] R. W. Ziolkowski and P. Jin, "Introduction of internal matching circuit to increase the bandwidth of a metamaterial-inspired efficient electrically small antenna," in *Proc. IEEE Int. Symp. Antennas Propag. and USNC/URSI National Radio Sci. Meeting*, San Diego, CA, Jul. 5–12, 2008, pp. 1–4.

[8] ECM Electronics, "ECM Axial Molded Choke MF Series Inductor Data Sheet," p. 2 [Online]. Available: http://www.chipinductors.co.uk/pdf/mf.PDF, (02/26/2008)

[9] muRata, "LQW21H_00 Series (0805 Size) Wire-Wound Ferrite Type Inductor Data Sheet," p. 51 [Online]. Available: http://www.murata.com/catalog/o05e18.pdf, (02/26/2008)